Carbohydrate Polymers 117 (2015) 312–318

Contents lists available at ScienceDirect

Carbohydrate Polymers

journal homepage: www.elsevier.com/locate/carbpol

Self-assembly and chiroptical property of poly(*N*-acryloyl-L-amino acid) grafted celluloses synthesized by RAFT polymerization

Yadong Liu [a], Xiaosa Jin [a,b], Xiaosa Zhang [a,b], Miaomiao Han [a], Shengxiang Ji [a,*]

[a] Key Laboratory of Polymer Ecomaterials, Changchun Institute of Applied Chemistry, Chinese Academy of Sciences, Changchun 130022, PR China
[b] University of Chinese Academy of Sciences, Beijing 100039, PR China

ARTICLE INFO

Article history:
Received 30 July 2014
Received in revised form 7 September 2014
Accepted 21 September 2014
Available online 7 October 2014

Keywords:
Cellulose
RAFT
Chiral polymers
Amino acid
Self-assembly

ABSTRACT

Three amphiphilic poly(*N*-acryloyl-L-amino acid) grafted celluloses were prepared by RAFT polymerization of *N*-acryloyl-L-amino acid, where amino acid is alanine, proline or glutamic acid, onto cellulose backbones. The chemical structure and solution properties of the brush copolymers were characterized with FTIR, NMR and wide angle X-ray diffraction (WAXD). The thermal stability of the brush copolymers was estimated by thermal gravimetric analysis (TGA). Circular dichroism (CD) and specific rotation measurements confirmed that these grafted celluloses had characteristic chiroptical properties. The amphiphilic brush copolymers self-assembled into micelles in the aqueous solution as confirmed by transmission electron microscopy (TEM) and dynamic light scattering (DLS) analyses. The micellar aggregates showed a tunable pH-responsive property and disaggregated to form unimolecular micelles at higher pH in diluted solutions. The brush copolymers have potential applications in controlled drug release and high-performance liquid chromatography, and so forth.

© 2014 Elsevier Ltd. All rights reserved.

1. Introduction

Cellulose is the most abundant biopolymer on earth (Wondraczek, Kotiaho, Fardim, & Heinze, 2011) and composed of several hundred to over ten thousand β-1, 4 linked D-glucose units, which imparts cellulose with unique physical and chemical properties. It has very attractive properties such as biodegradability, renewability, high strength and modulus (Lucia & Hubbe, 2008; Pandey et al., 2005). Recently, there is a growing interest in cellulose-based brush polymers because they can self-assemble into micelles with diameters ranging between 10 and 100 nm (Hassani, Hendra, & Bouchemal, 2012; Wang et al., 2011). These self-assembled micelles have potential applications in sensing (Wang, Guo, Li, Chen, & Sun, 2012), bioimaging and drug delivery (Chen et al., 2011). However, the extremely poor solubility of cellulose in water and many common organic solvents is the main obstacle for its chemical functionalization (Klemm, Heublein, Fink, & Bohn, 2005; Peng, Ren, Zhong, & Sun, 2011). Hence, most cellulose-base brush polymers were prepared from soluble cellulose derivatives (acetate cellulose (Luo et al., 2013), ethyl cellulose (EC) (Kim et al., 2006; Yan et al., 2009), hydroxypropyl cellulose (Jin, Kang, Liu, & Huang, 2013) and hydroxyethylcellulose (Fenn & Heinze, 2009; Yang, Wang, & Zhou, 2007)).

Among the cellulose derivatives, modification by grating synthetic polymers has been an effective method to develop cellulose-based hybrid materials (Song, Zhou, Li, Lue, & Zhang, 2009; Xu et al., 2013). Ring-opening polymerization (ROP) (Habibi et al., 2008), atom transfer radical polymerization (ATRP) (Carlmark & Malmstrom, 2003) and click chemistry (Krouit, Bras, & Belgacem, 2008) are three widely used grafting methods for cellulose modification. Significant efforts have been devoted to graft polymerization of different kinds of monomers, such as styrene (Vlcek et al., 2008), acrylamide (Hiltunen, Raula, & Maunu, 2011), *N*-isopropylacrylamide (Ifuku & Kadla, 2008; Liu, Kang, & Huang, 2013), methyl methacrylate (Yamanaka, Teramoto, & Nishio, 2013), butyl acrylate (Kang et al., 2006), L-lactide (Dong et al., 2008) and ε-caprolactone (Guo, Wang, Shen, Shu, & Sun, 2013), from cellulose backbones by ATRP or ROP. These grafted copolymers consisted of semi-rigid cellulose backbones and flexible side chains, which were found to have some interesting properties like pH and thermal response, liquid crystalline behavior and antibacterial activity. Liu, Liu, Zeng, Liu, and Huang, (2012) studied the conformation transition of EC-*graft*-poly(acrylic acid) via tuning the brush density. Disclike and rodlike micelles were obtained from sparsely- and densely-grafted copolymers, respectively. Yuan, Zhang, Zou, Shen, and Ren (2012) synthesized ethyl cellulose brush copolymer, EC-*graft*-poly(2-(2-methoxyethoxy)ethyl

* Corresponding author. Tel.: +86 43185262286.
E-mail address: sji@ciac.ac.cn (S. Ji).

http://dx.doi.org/10.1016/j.carbpol.2014.09.074
0144-8617/© 2014 Elsevier Ltd. All rights reserved.

methacrylate)-co-oligo(ethylene glycol) methacrylate), by the combination of ATRP and click chemistry and the brush copolymer showed response to the change of temperature and pH. However, there are no reports on poly(amino acid)-grafted celluloses.

Amino-acid based polymers can be divided into two groups, depending on whether the amino acid moieties are borne in the main chain or side chain (Sanda & Endo, 1999). Most synthetic polypeptides containing amino acid moieties in the main chain are obtained by ring-opening polymerization of *N*-carboxy-α-amino acid anhydrides (Fujita et al., 2007; He et al., 2008). In recent years, much interest has been also devoted to preparing well-defined polymers having amino-acid substituents in the side chains, which have been synthesized by free radical polymerization of vinyl monomer carrying amino acid residues. Comparing with the synthetic polypeptides, it is convenient to control the sequence and composition of amino acids, chain chirality, amphiphilicity and chain length. McCormick and coworkers (Lokitz et al., 2006) reported the synthesis of well-defined homopolymers, random copolymers, and block copolymers of enantiomeric amino acid acrylates, *N*-acryloyl-L-alanine (A-(L)Ala-OH) and *N*-acryloyl-D-alanine, via the RAFT process. Du, Willcock, Ieong, and O'Reilly, (2011) studied amphiphilic poly(2-(diethylamino)ethyl methacrylate)-*b*-poly(*N*-acryloyl-L-phenylalanine) block copolymers, the copolymers were chiral and had response to pH change. Although poly(*N*-acryloyl-L-amino acid)-based side-chain polymers have been intensively investigated, brush copolymers with cellulose backbones have never been considered.

In this paper, novel cellulose brush copolymers were prepared by grafting poly(*N*-acryloyl-L-amino acid) via RAFT polymerization of amino acid acrylates. The cellulose was first modified with S-1-dodecyl-S′-(α,α′-dimethyl-α″-acetic acid)trithiocarbonate to obtain cellulose based chain transfer agent (Cell-CTA). Poly(*N*-acryloyl-L-amino acid)-grafted celluloses were synthesized by graft polymerization of different amino acid acrylate monomers, (A-(L)Ala-OH), *N*-acryloyl-L-proline (A-(L)Pro-OH) and *N*-acryloyl-L-glutamic acid (A-(L)Glu-OH)), at 80 °C, respectively, and characterized by ^{1}HNMR, XRD, TGA, CD and specific rotation techniques.

2. Experimental

2.1. Materials

L-Alanine, L-proline, L-glutamic acid and acryloyl chloride were purchased from Aladdin and used as received. Cellulose (powder, cotton linters) was obtained from Sigma Aldrich (product no. C6288) and dried at 140 °C for 2 h under vacuum before use. 2,2′-Azobis(isobutyronitrile) (AIBN) was purified by recrystallization from methanol. Chain transfer agent (CTA), S-1-dodecyl-S′-(α,α′-dimethyl-α″-acetic acid)trithiocarbonate, was synthesized according to the reported procedure (Lai, Filla, & Shea, 2002). *N*, *N*′-dimethylacetamide (DMAc) and tetrahydrofuran (THF) were distilled after CaH_2 treatment. All other materials were used without further purification.

2.2. Measurement

^{1}HNMR and ^{13}CNMR spectra were recorded on a Bruker AV 300 NMR spectrometer in deuterium oxide (D_2O), chloroform-d ($CDCl_3$) and dimethyl sulfoxide-d_6 (DMSO-d_6). Fourier transform infrared spectrometer (FT-IR) spectra of the samples were recorded on a Bio-Rad Win-IR instrument in the range of 4000–500 cm^{-1}. Gel permeation chromatography (GPC) measurements were carried out at 35 °C with a Waters 1515 GPC instrument and Waters 2414 refractive index detector. Water was used as the eluent at a flow rate of 1 mL min^{-1}. The molecular weights were calibrated with polyethylene glycol (PEG) standards. Circular dichroism (CD) analysis was performed with a JASCO J810 spectrometer at room temperature with alkaline water (pH = 11.0) as solvent. Specific rotations were measured by a Jasco Polarimeter (Japan). The wide angle X-ray diffraction (WAXD) data from 5° to 40° were measured using a Rigaku D/max 2500 kVPC X-Ray Diffractometer with a Cu tube anode. The thermal stability was estimated by thermal gravimetric analysis (TGA) (TA Instrument Q500) under a nitrogen atmosphere. The measurements were performed incrementally (10 °C/min) from 50 °C up to 700 °C. The size distribution of micelles was determined by dynamic light scattering (DLS) techniques. The experiments were performed on a vertically polarized He–Ne laser (DAWN EOS, Wyatt Technology). Transmission electron microscopy (TEM) was performed on a JEOL JEM-1011 electron microscope, and the measurements were performed at an accelerating voltage of 100 kV.

2.3. Synthesis of monomers

A-(L)Ala-OH, A-(L)Pro-OH and A-(L)Glu-OH were prepared by coupling acryloyl chloride with their respective amino acids (Scheme S1). A representative procedure for the synthesis of *N*-acryloyl-L-alanine was given as an example. L-alanine (3.0 g, 33.7 mmol) was dissolved in 80 mL 1.25 M NaOH aqueous solution and an equimolar of acryloyl chloride (3.0 g, 33.1 mmol) was added into the solution dropwise at 0 °C. The mixture was stirred for 2 h at room temperature, acidified with 12 N HCl, and then extracted with ethyl acetate three times. The combined organic phase was dried over anhydrous $MgSO_4$. After filtration, the filtrate was concentrated under reduced pressure. The solid was recrystallized three times from ethyl acetate to give 2.9 g of *N*-acryloyl-L-alanine (60.2%). The NMR spectra of A-(L)Ala-OH, A-(L)Pro-OH and A-(L)Glu-OH were shown in Fig. S1.

2.4. Synthesis of CTACl

CTA (4.5 g, 12.4 mmol) was introduced into a dried Schlenk flask and dissolved in anhydrous dichloromethane. Oxalyl chloride (1.2 mL, 12.6 mmol) was added dropwise to the CTA mixture solution at room temperature and the reaction mixture was refluxed for 7 h. The solvent and unreacted oxalyl chloride were removed under vacuum at room temperature to yield a yellow and highly viscous liquid (CTACl, 4.7 g, 98.8%).

2.5. Synthesis of cellulose based macroinitiator (Cell-CTA)

Dry cellulose (1.0 g, AUG 6.17 mmol) was suspended in 40 mL of DMAc, and the mixture was heated at 150 °C for 2 h. After the slurry was cooled to 80 °C, 2.65 g of anhydrous LiCl was added and the mixture was stirred at 80 °C for 10 h. Cellulose completely dissolved after the mixture was cooled down to room temperature under stirring. After the addition of triethylamine (1.37 g, 13.5 mmol) into the cellulose solution at room temperature, the mixture was cooled below 10 °C. CTACl (4.7 g, 12.3 mmol) in 2 mL of DMAc was added dropwise into the above cellulose solution over 30 min. After addition, the mixture was stirred for additional 24 h at room temperature and then precipitated into methanol. The precipitate was dissolved in $CHCl_3$ and reprecipitated in methanol. The precipitation process was repeated three times to give 4.1 g (81.8%) of Cell-CTA.

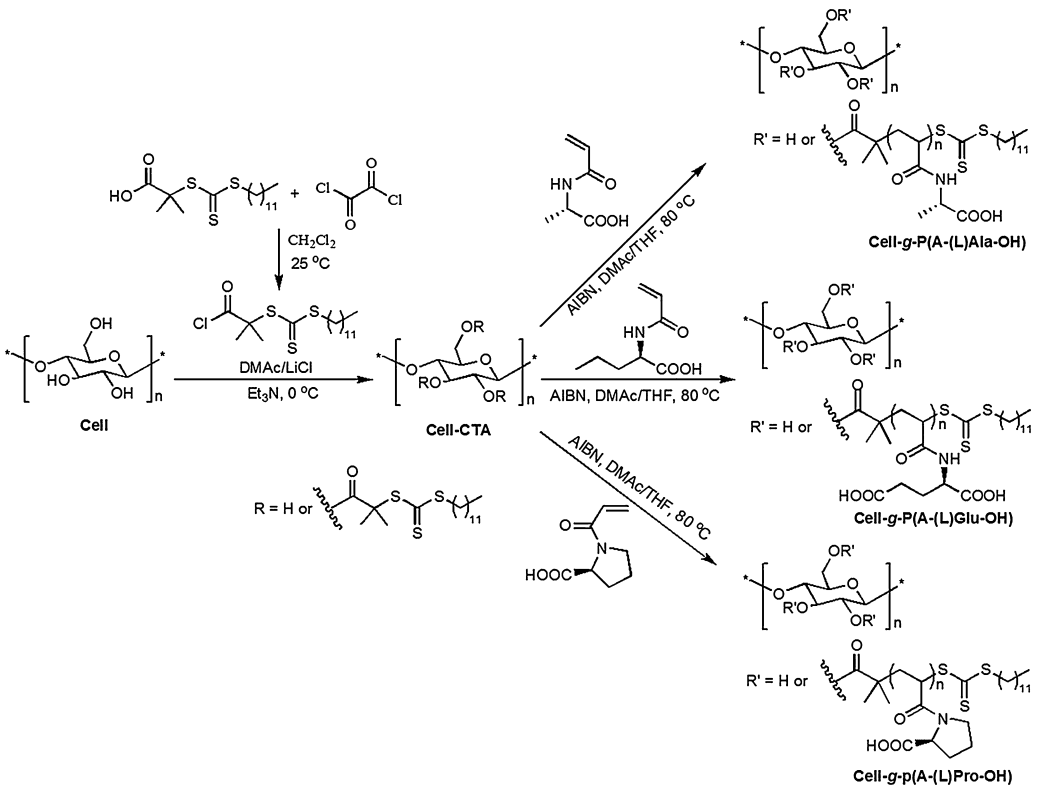

Scheme 1. Synthesis of poly(*N*-acryloyl-L-amino acid) grafted celluloses.

2.6. Synthesis of graft copolymers by RAFT polymerization of A-(L)Ala-OH, A-(L)Pro-OH and A-(L)Glu-OH using Cell-CTA as macroinitiators

The procedure for synthesis of Cell-*g*-P(A-(L)Ala-OH) was given as an example (Scheme 1). Cell-CTA (50 mg, CTA 0.11 mmol) and AIBN (2.70 mg, 0.016 mmol) were first dissolved in 10 mL of THF. The solution was then added into A-(L)Ala-OH (1.0 g, 6.99 mmol) in DMAc (10 mL). The mixed solution was degassed by three freeze-thaw cycles. The polymerization was performed at 80 °C for 10 h under nitrogen. After removal of THF by evaporation, the crude product was precipitated in diethyl ether with vigorous stirring. The precipitate was dissolved in methanol and dialyzed against methanol for 4 days using the dialysis membrane (cut-off M_W = 7000 g/mol). The solution was concentrated and precipitated into diethyl ether to yield a slightly yellow solid (0.7 g, 66.7%)

2.7. Cleavage of poly(N-acryloyl-L-amino acid) side chains

A representative protocolis as follows, Cell-*g*-P(A-(L)Ala-OH) (100 mg) was treated with a 2 N solution of HCl in methanol at 37 °C for 48 h. The resulting mixture was dialyzed against H_2O for 4 days using dialysis membrane to remove HCl. After the water was evaporated, the resultant solid was washed twice with methanol (5 mL). Methanol was removed by under vacuum at 50 °C to give 38 mg of poly(*N*-acroyloyl-L-amino acid). The molecular weight of the side chain P(A-(L)Ala-OH) was 4800 g/mol with a PDI of 1.41 as analyzed by GPC.

2.8. Preparation of self-assembled micelles of brush copolymers

Brush copolymer (10 mg) was added into an aqueous NaOH solution (100 mL) at pH = 10 and the solution turned to clear after being stirred for 30 min and sequentially stirred for 24 h for TEM and DLS measurement. For different measurements, the micelle solutions can be diluted to different concentrations by basic aqueous solution at pH = 12.8 and equilibrated at 25 °C for 24 h for DLS measurement.

3. Results and discussion

3.1. Synthesis and characterization of cellulose brush copolymers by RAFT

Cellulose brush copolymers with side chains of P(A-(L)Ala-OH), P(A-(L)Glu-OH) and P(A-(L)Pro-OH) were prepared via RAFT polymerization of A-(L)Ala-OH, A-(L)Glu-OH and A-(L)Pro-OH, respectively. The procedure for the synthesis of cellulose brush copolymers is shown in Scheme 1. Cell-CTA was synthesized by modification of cellulose through the coupling of the hydroxyl group with CTACl under moderate conditions. The formation of Cell-CTA was confirmed by FT-IR, ^{1}HNMR and ^{13}CNMR analyses. Fig. S2 shows FT-IR spectra of both Cell-CTA and original cellulose. A new absorption peak at 1742 cm^{-1} in the FT-IR spectrum was attributed to the formation of ester bonds after the coupling reaction. ^{1}HNMR spectra of Cell-CTA was shown in Fig. 1. Signals corresponding to the protons of CTA (Fig. S3, signal "a–e") and the cellulose protons (Fig. 1, signal "1–6") were observed in the spectrum of Cell-CTA, which confirmed the formation of the CTA ester. The ^{13}C NMR spectrum also confirmed the formation of Cell-CTA (Fig. S3). The degree of substitution (DS) of Cell-CTA was 1.52 (Table 1) and the quantification protocol was detailed in Supporting Information.

Graft polymerization of *N*-acryloyl-L-amino acid from Cell-CTA macroinitiators was performed at 80 °C under a nitrogen atmosphere. A mixed solvent of THF and DMAc (1:1) was used due to the different solubilities of Cell-CTA and *N*-acryloyl-L-amino acid. Cell-CTA and AIBN were first dissolved in THF. Subsequently, the solution was slowly added into the DMAc solution of *N*-acryloyl-L-amino acid. The compositions of the cellulose brush

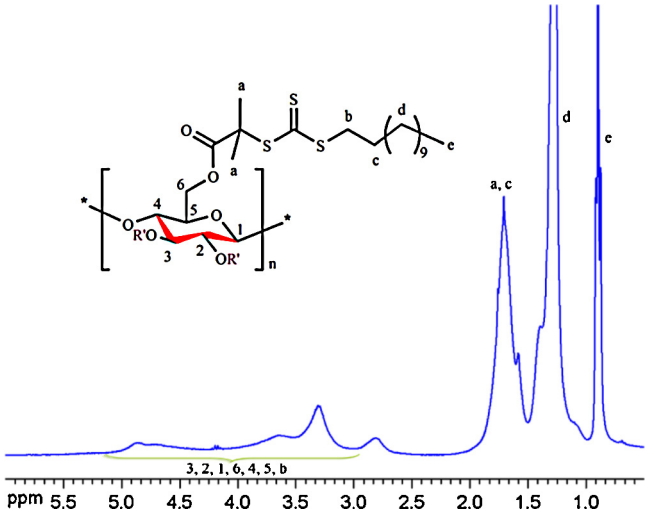

Fig. 1. ^{1}HNMR spectrum of Cell-CTA.

Table 1
Characterization of poly(*N*-acryloyl-L-amino acid) grafted celluloses.

Copolymer	Cell-*g*-P(A-(L)Ala-OH)	Cell-*g*-P(A-(L)Glu-OH)	Cell-*g*-P(A-(L)Pro-OH)
DS[a]	1.52	1.52	1.52
$M_{n,side\ chain}$[b]	4.8k	4.8k	5.1k
PDI (M_w/M_n)[b]	1.41	1.62	1.35
Decomposition temperature (°C)[c]	243.4	224.7	257.1
$[\alpha]_D^{25}$ (deg)[d]	−48.7	−14.1	−69.5
Color	Pale yellow	Pale yellow	Pale yellow

[a] Determined by ^{1}HNMR (see Supporting Information).
[b] Determined by GPC in H_2O, relative to PEG standard.
[c] Determined by TGA from 50 to 700 °C.
[d] Measured at a concentration of 0.2 g/dL in methanol at 25 °C.

copolymers prepared from different *N*-acryloyl-L-amino acid are summarized in Table 1. Fig. 2 shows the ^{1}HNMR spectra of Cell-*g*-P(A-(L)Ala-OH), Cell-*g*-P(A-(L)Glu-OH) and Cell-*g*-P(A-(L)Pro-OH). The disappearance of vinylic proton signal and the appearance of poly(*N*-acryloyl-L-amino acid) proton signal at about 1.85 ppm (Fig. 2, signal "a–b") confirmed the grafting of poly(*N*-acryloyl-L-amino acid) onto celluloses. The molecular weights of grafted side chains were measured to be ~4.8–5.1 kg/mol by GPC after being cleaved from cellulose and summarized in Table 1. The solubility results for Cell-CTA, Cell-*g*-P(A-(L)Ala-OH), Cell-*g*-P(A-(L)Glu-OH) and Cell-*g*-P(A-(L)Pro-OH) are summarized in Table S1. All the poly(*N*-acryloyl-L-amino acid)-grafted celluloses exhibited excellent solubility in most of organic solvents, such as DMSO, DMF and ethanol.

All cellulose brush copolymers are composed of chiral cellulose backbones and chiral side chains and are optically active (Table 1). They were regarded as chiral–chiral type brush polymers. The cellulose brush copolymers based on different amino acids exhibited different specific rotations, due to the different monomer and polymer structures. Circular dichroism (CD) spectroscopy was empolyed for chiroptical characterization of the cellulose brush copolymers. The CD spectra of the cellulose brush copolymers in basic water (pH = 11, polymer concentration = 0.33 mg/mL) are shown in Fig. 3. Cell-*g*-P(A-(L)Pro-OH) showed a negative signal at 208 nm and a positive signal at 237 nm, which were probably attributed to the $n \rightarrow \pi^*$ transition of carboxyl chromophore and the $\pi_1 \rightarrow \pi^*$ transition of amide chromophore, respectively (Morcellet-Sauvage, Morcellet, & Loucheux, 1983). Cell-*g*-P(A-(L)Ala-OH) and Cell-*g*-P(A-(L)Glu-OH) both showed a positive

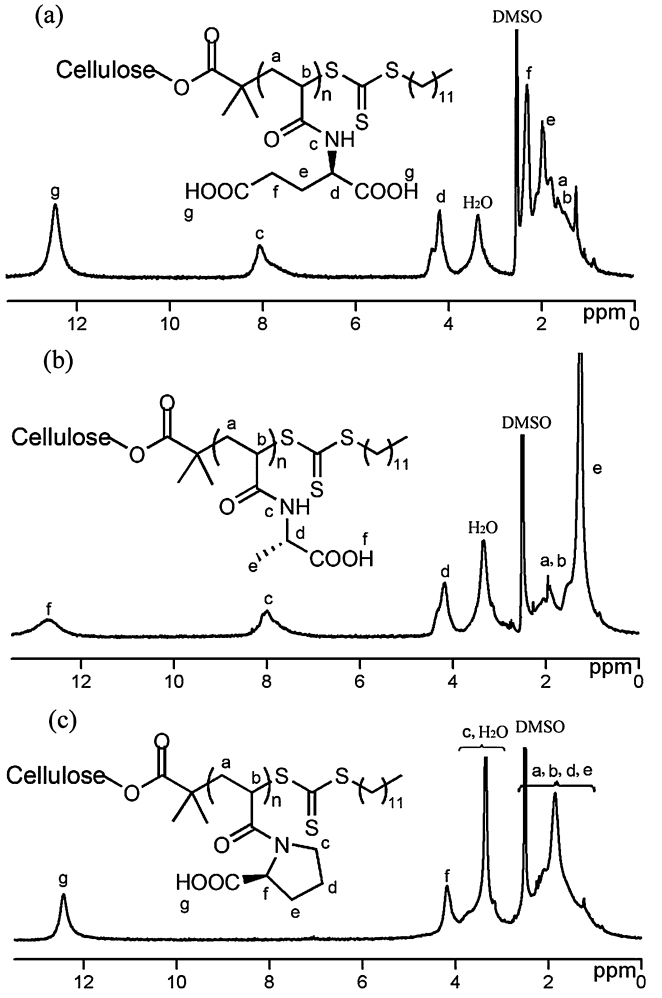

Fig. 2. ^{1}HNMR (300 MHz, in DMSO-d_6) of poly(*N*-acryloyl-L-amino acid) grafted celluloses.

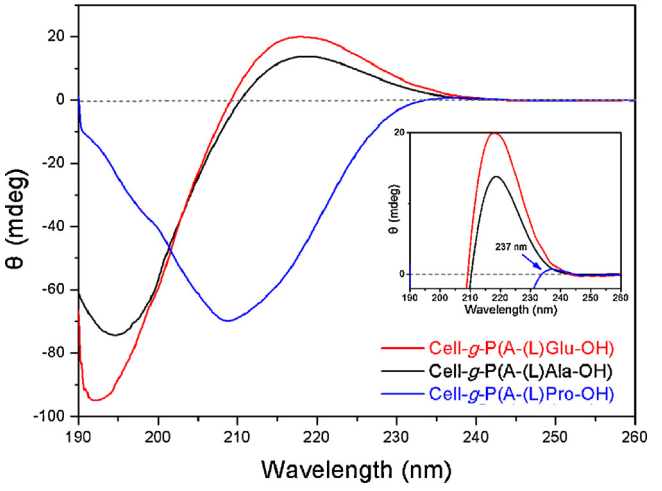

Fig. 3. CD spectra of poly(*N*-acryloyl-L-amino acid) grafted celluloses in water (pH = 11).

signal at 218 nm, which are generally assigned to the $\pi_1 \rightarrow \pi^*$ transition of amide chromophore. However, Cell-*g*-P(A-(L)Ala-OH) and Cell-*g*-P(A-(L)Glu-OH) possessed negative signals at 196 and 194 nm, respectively, which were generally due to the $n \rightarrow \pi^*$ transition of carboxyl chromophore. The results suggested that

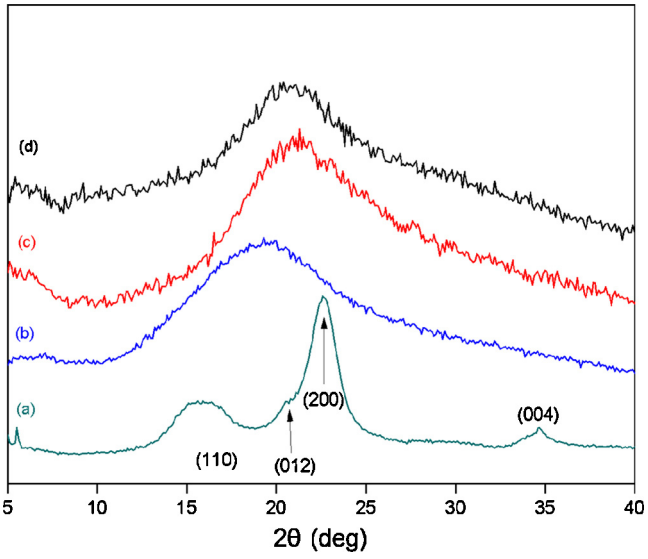

Fig. 4. X-ray diffraction patterns of (a) cellulose, (b) Cell-*g*-P(A-(L)Pro-OH), (c) Cell-*g*-P(A-(L)Glu-OH) and (d) Cell-*g*-P(A-(L)Ala-OH).

Cell-*g*-P(A-(L)Pro-OH) had different conformation from Cell-*g*-P(A-(L)Ala-OH) and Cell-*g*-P(A-(L)Glu-OH) in basic water.

The wide angle X-ray diffraction of Cell-*g*-P(A-(L)Ala-OH), Cell-*g*-P(A-(L)Glu-OH) and Cell-*g*-P(A-(L)Pro-OH) was performed at room temperature in the region of $2\theta = 5–40^\circ$ as illustrated in Fig. 4. Cellulose had four characteristic peaks at 2θ angles of 16.8°, 20.8°, 22.6° and 34.7°, corresponding to (1 1 0), (0 1 2), (2 0 0) and (0 0 4) crystallographic planes(cottonSebe, Ham-Pichavant, Ibarboure, Koffi, & Tingaut, 2012; Isogai, Usuda, Kato, Uryu, & Atalla, 1989), respectively. Whereas, for Cell-*g*-P(A-(L)Ala-OH), Cell-*g*-P(A-(L)Glu-OH) and Cell-*g*-P(A-(L)Pro-OH), there were a broad peak in the 2θ angles of 10–30° region, indicating that Cell-*g*-P(A-(L)Ala-OH), Cell-*g*-P(A-(L)Glu-OH) and Cell-*g*-P(A-(L)Pro-OH) were amorphous. This may be ascribed to the introduction of bulky pendent chains in cellulose matrix which destroyed the 3D structure of cellulose, resulting in low crystallinity of the cellulose brush copolymers. Fig. S4 shows the TGA curves of the cellulose brush polymers, and the TGA curve of pure cellulose showed single stage decomposition with the onset of weight loss at about 320 °C. The cellulose-based brush copolymers clearly had two decomposition stages. The first weight loss step occurred in the temperature from 220 to 260 °C, which might be attributed to the degradation of poly(*N*-acroyloyl-L-amino acid) side chains. The subsequent loss step should be due to the decomposition of cellulose. The decomposition temperature of the cellulose-based brush copolymers is summarized in Table 1.

3.2. Self-assembly of cellulose based amphiphilic brush copolymers

Self-assembly of Cell-*g*-P(A-(L)Ala-OH), Cell-*g*-P(A-(L)Glu-OH) and Cell-*g*-P(A-(L)Pro-OH) was performed in aqueous NaOH solutions. The hydrodynamic radii (R_h) of self-assembled micelles were characterized by DLS (Fig. 5A). At pH = 10, DLS results showed these polymers self-assembled into micelles with R_h of 45 ± 8 nm, 78 ± 8 nm and 120 ± 11 nm for Cell-*g*-P(A-(L)Ala-OH), Cell-*g*-P(A-(L)Glu-OH) and Cell-*g*-P(A-(L)Pro-OH), respectively. The R_hs of these micelles decreased to 25 ± 4 nm, 39 ± 5 nm and 33 ± 4 nm, respectively, with the increase of the pH value to 11. When the pH value was increased to 12.8, the R_h value of Cell-*g*-P(A-(L)Glu-OH) slightly decreased while the R_h values did not change for Cell-*g*-P(A-(L)Ala-OH) and Cell-*g*-P(A-(L)Pro-OH). The R_h values did not change with further dilution of the solution concentrations from 0.01 mg/mL to 0.0001 mg/mL (Fig. 5B), which confirmed the formation of unimolecular micelles at pH = 12.8. On the other hand, adjusting the pH value to 9 by the addition of diluted HCl solution led to the re-aggregation of micelles to precipitate from the solution.

The morphologies of self-assembled brush copolymers in basic aqueous solution were characterized by TEM. Fig. 6a–c showed TEM images of Cell-*g*-P(A-(L)Ala-OH), Cell-*g*-P(A-(L)Glu-OH) and Cell-*g*-P(A-(L)Pro-OH) micelles at pH = 10.0. The spheroid morphology of the brush copolymers micelles was clearly visible. The R_h values of the spherical micelles were measured to be 64 ± 13, 81 ± 21 and 115 ± 16 nm for Cell-*g*-P(A-(L)Ala-OH), Cell-*g*-P(A-(L)Glu-OH) and Cell-*g*-P(A-(L)Pro-OH), respectively, consistent with the trend from the DLS measurement. Similarly, TEM measurement also confirmed that the sizes of the micelles decreased when the pH value was increased from 10 to 12.8 (Fig. 6e–f).

Both DLS and TEM measurements showed that the self-assembly behaviors of these three polymers responded to the change of the solution's pH value. At a lower pH, these polymers might be partially ionized and aggregate to form micelles of larger sizes. At a higher pH, all carboxylic acid groups on side chains might be fully ionized and the electronic repulsion might be the reason for

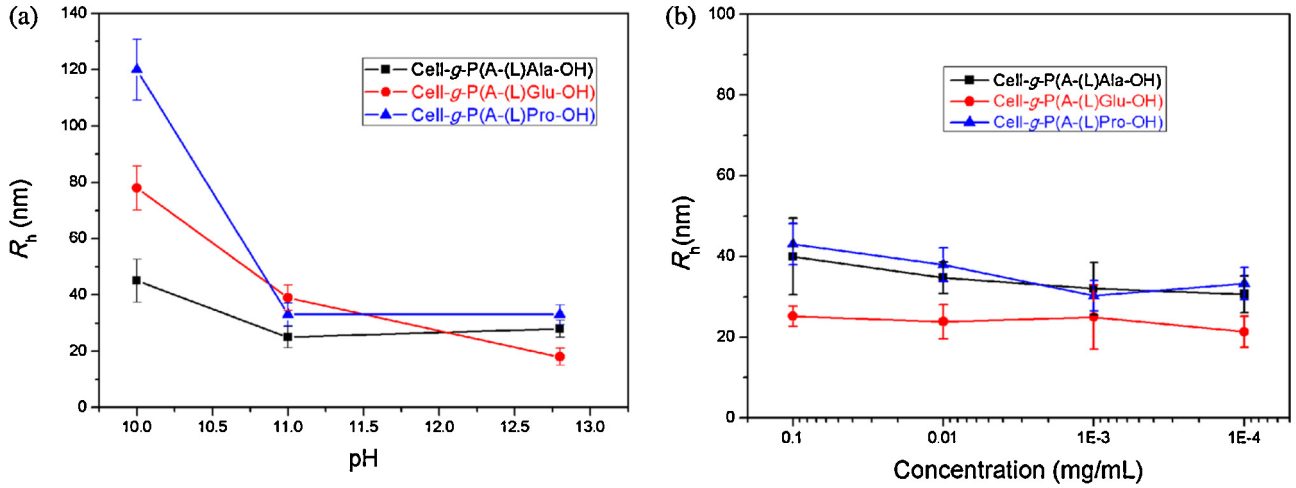

Fig. 5. (a) pH dependence of R_h of the micelles of poly(*N*-acryloyl-L-amino acid) grafted celluloses and (b) the effect of dilution on R_h of the micelles of poly(*N*-acryloyl-L-amino acid) grafted celluloses at pH = 12.8.

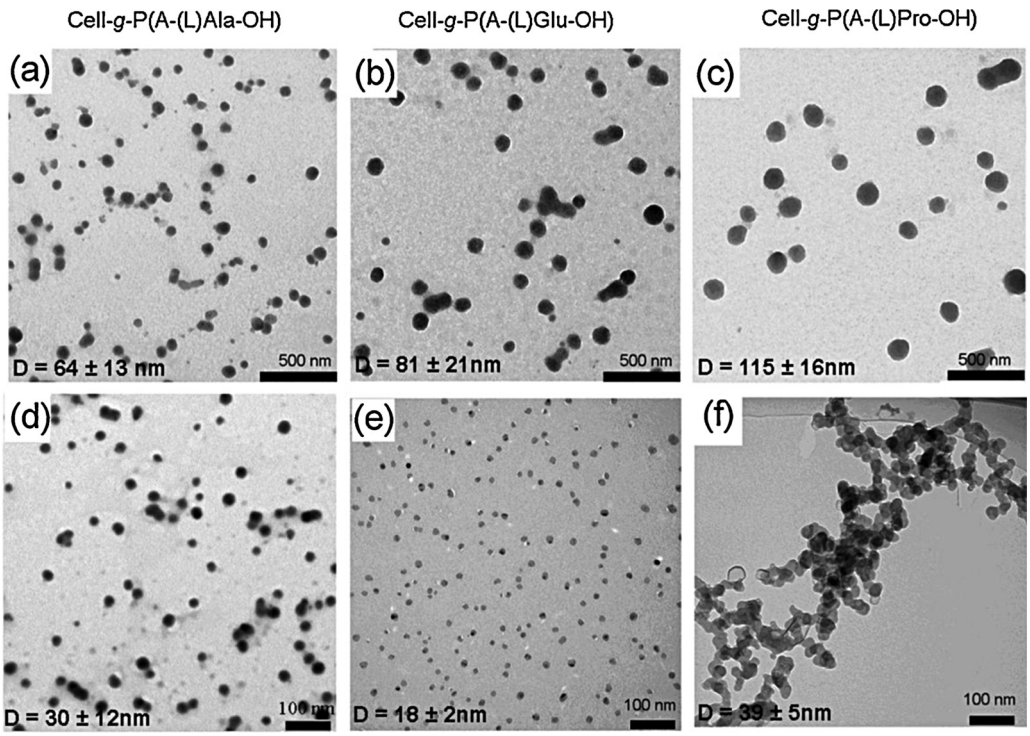

Fig. 6. TEM photographs of different poly(*N*-acryloyl-L-amino acid) grafted celluloses at the aqueous solution at different pH values: (a)–(c) pH = 10 and (d)–(f) pH = 12.8.

the full dissolution of the polymeric aggregates to form unimolecular micelles. Compares to linear block copolymers, the formation of unimolecular micelles is a unique property of amphiphilic brush copolymers, which might find potential applications in drug delivery and tissue engineering.

4. Conclusion

Three cellulose brush copolymers, Cell-*g*-P(A-(L)Ala-OH), Cell-*g*-P(A-(L)Glu-OH) and Cell-*g*-P(A-(L)Pro-OH), were synthesized by RAFT polymerization of A-(L)Ala-OH, A-(L)Glu-OH and A-(L)Pro-OH, respectively, using Cell-CTA macroinitiator in a mixed solvent. These amphiphlic cellulose brush copolymers self-assembled into spherical micelles in aqueous solution and the sizes of micelles were sensitive to pH values of the media as confirmed by TEM and DLS analyses. At high pH, the micelles disaggregated to form unimolecular micelles in diluted solutions. The pH-responsive self-assembly behavior of these materials might result in potential application in drug delivery. Since both the backbone and side chains were chiral, these coplymers showed characteristic chiroptical properties, which could be useful as the chiral stationary phase for HPLC. The nature of amino acid and cellulose makes these cellulose brush copolymers to be environmentally friendly.

Acknowledgment

This project was financially supported by the National Natural Science Foundation of China (Project nos. 51203154 and 51303175) and "The Hundred Talents Program" from the Chinese Academy of Sciences.

Appendix A. Supplementary data

Supplementary material related to this article can be found, in the online version, at http://dx.doi.org/10.1016/j.carbpol.2014.09.074.

References

Carlmark, A., & Malmstrom, E. E. (2003). ATRP grafting from cellulose fibers to create block-copolymer grafts. *Biomacromolecules*, *4*(6), 1740–1745.

Chen, C. H., Cuong, N. V., Chen, Y. T., So, R. C., Liau, I., & Hsieh, M. F. (2011). Overcoming multidrug resistance of breast cancer cells by the micellar doxorubicin nanoparticles of mPEG-PCL-graft-cellulose. *Journal of Nanoscience and Nanotechnology*, *11*(1), 53–60.

cottonSebe, G., Ham-Pichavant, F., Ibarboure, E., Koffi, A. L., & Tingaut, P. (2012). Supramolecular structure characterization of cellulose II nanowhiskers produced by acid hydrolysis of cellulose I substrates. *Biomacromolecules*, *13*(2), 570–578.

Dong, H. Q., Xu, Q., Li, Y. Y., Mo, S. B., Cai, S. J., & Liu, L. J. (2008). The synthesis of biodegradable graft copolymer cellulose-graft-poly(L-lactide) and the study of its controlled drug release. *Colloids and Surfaces B – Biointerfaces*, *66*(1), 26–33.

Du, J., Willcock, H., Ieong, N. S., & O'Reilly, R. K. (2011). pH-responsive chiral nanostructures. *Australian Journal of Chemistry*, *64*(8), 1041–1046.

Fenn, D., & Heinze, T. (2009). Novel 3-mono-O-hydroxyethyl cellulose: Synthesis and structure characterization. *Cellulose*, *16*(5), 853–861.

Fujita, Y., Koga, K., Kim, H. K., Wang, X. S., Sudo, A., Nishida, H., et al. (2007). Phosgene-free synthesis of N-carboxyan hyd rides of alpha-amino acids based on bisarylcarbonates as starting compounds. *Journal of Polymer Science Part A – Polymer Chemistry*, *45*(22), 5365–5369.

Guo, Y., Wang, X., Shen, Z., Shu, X., & Sun, R. (2013). Preparation of cellulose-graft-poly(varepsilon-caprolactone) nanomicelles by homogeneous ROP in ionic liquid. *Carbohydrate Polymers*, *92*(1), 77–83.

Habibi, Y., Goffin, A. L., Schiltz, N., Duquesne, E., Dubois, P., & Dufresne, A. (2008). Bionanocomposites based on poly(epsilon-caprolactone)-grafted cellulose nanocrystals by ring-opening polymerization. *Journal of Materials Chemistry*, *18*(41), 5002–5010.

Hassani, L. N., Hendra, F., & Bouchemal, K. (2012). Auto-associative amphiphilic polysaccharides as drug delivery systems. *Drug Discovery Today*, *17*(11–12), 608–614.

He, C. L., Zhao, C. W., Guo, X. H., Guo, Z. J., Chen, X. S., Zhuang, X. L., et al. (2008). Novel temperature- and pH-responsive graft copolymers composed of poly(L-glutamic acid) and poly(N-isopropylacrylamide). *Journal of Polymer Science Part A – Polymer Chemistry*, *46*(12), 4140–4150.

Hiltunen, M. S., Raula, J., & Maunu, S. L. (2011). Tailoring of water-soluble cellulose-g-copolymers in homogeneous medium using single-electron-transfer living radical polymerization. *Polymer International*, *60*(9), 1370–1379.

Ifuku, S., & Kadla, J. F. (2008). Preparation of a thermosensitive highly regioselective cellulose/N-isopropylacrylamide copolymer through atom transfer radical polymerization. *Biomacromolecules*, *9*(11), 3308–3313.

Isogai, A., Usuda, M., Kato, T., Uryu, T., & Atalla, R. H. (1989). Solid-state CP/MAS C-13 NMR-study of cellulose polymorphs. *Macromolecules*, *22*(7), 3168–3172.

Jin, X., Kang, H. L., Liu, R. G., & Huang, Y. (2013). Regulation of the thermal sensitivity of hydroxypropyl cellulose by poly(N-isopropylacryamide) side chains. *Carbohydrate Polymers*, *95*(1), 155–160.

Kang, H., Liu, W., He, B., Shen, D., Ma, L., & Huang, Y. (2006). Synthesis of amphiphilic ethyl cellulose grafting poly(acrylic acid) copolymers and their self-assembly morphologies in water. *Polymer*, *47*(23), 7927–7934.

Kim, M. S., Hyun, H., Seo, K. S., Cho, Y. H., Lee, J. W., Lee, C. R., et al. (2006). Preparation and characterization of MPEG-PCL diblock copolymers with thermo-responsive sol–gel–sol phase transition. *Journal of Polymer Science Part A – Polymer Chemistry*, *44*(18), 5413–5423.

Klemm, D., Heublein, B., Fink, H. P., & Bohn, A. (2005). Cellulose: Fascinating biopolymer and sustainable raw material. *Angewandte Chemie-International Edition*, *44*(22), 3358–3393.

Krouit, M., Bras, J., & Belgacem, M. N. (2008). Cellulose surface grafting with polycaprolactone by heterogeneous click-chemistry. *European Polymer Journal*, *44*(12), 4074–4081.

Lai, J. T., Filla, D., & Shea, R. (2002). Functional polymers from novel carboxyl-terminated trithiocarbonates as highly efficient RAFT agents. *Macromolecules*, *35*, 6754–6756.

Liu, R., Kang, H., & Huang, Y. (2013). Synthesis of ethyl cellulose grafted poly(N-isopropylacrylamide) copolymer and its micellization. *Acta Chimica Sinica*, *71*, 114–120.

Liu, W., Liu, Y., Zeng, G., Liu, R., & Huang, Y. (2012). Coil-to-rod conformational transition and single chain structure of graft copolymer by tuning the graft density. *Polymer*, *53*, 1005–1014.

Lokitz, B. S., Convertine, A. J., Ezell, R. G., Heidenreich, A., Li, Y. T., & McCormick, C. L. (2006). Responsive nanoassemblies via interpolyelectrolyte complexation of amphiphilic block copolymer micelles. *Macromolecules*, *39*(25), 8594–8602.

Lucia, L. A., & Hubbe, M. A. (2008). Book review: Materials, chemicals & energy from forest biomass. *Bioresources*, *3*(3), 668–669.

Luo, Y., Wang, S., Shen, M., Qi, R., Fang, Y., Guo, R., et al. (2013). Carbon nanotube-incorporated multilayered cellulose acetate nanofibers for tissue engineering applications. *Carbohydrate Polymers*, *91*(1), 419–427.

Morcellet-Sauvage, J., Morcellet, M., & Loucheux, C. (1983). Poly(methacrylic acid) derivatives. 7. Chiroptical properties of optically active poly(N-methacryloyl-L-alanine) and poly(N-methacryloyl-L-alanine-co-L-phenylmethacrylamide). *Macromolecules*, *16*(10), 1564–1570.

Pandey, J. K., Kumar, A. P., Misra, M., Mohanty, A. K., Drzal, L. T., & Singh, R. P. (2005). Recent advances in biodegradable nanocomposites. *Journal of Nanoscience and Nanotechnology*, *5*(4), 497–526.

Peng, X. W., Ren, J. L., Zhong, L. X., & Sun, R. C. (2011). Homogeneous synthesis of hemicellulosic succinates with high degree of substitution in ionic liquid. *Carbohydrate Polymers*, *86*(4), 1768–1774.

Sanda, F., & Endo, T. (1999). Syntheses and functions of polymers based on amino acids. *Macromolecular Chemistry and Physics*, *200*(12), 2651–2661.

Song, Y. B., Zhou, J. P., Li, Q., Lue, A., & Zhang, L. N. (2009). Solution properties of the acrylamide-modified cellulose polyelectrolytes in aqueous solutions. *Carbohydrate Research*, *344*(11), 1332–1339.

Vlcek, P., Janata, M., Latalova, P., Dybal, J., Spirkova, M., & Toman, L. (2008). Bottlebrush-shaped copolymers with cellulose diacetate backbone by a combination of ring opening polymerization and ATRP. *Journal of Polymer Science Part A – Polymer Chemistry*, *46*(2), 564–573.

Wang, D. Q., Tan, J. J., Kang, H. L., Ma, L., Jin, X., Liu, R. G., et al. (2011). Synthesis, self-assembly and drug release behaviors of pH-responsive copolymers ethyl cellulose-graft-PDEAEMA through ATRP. *Carbohydrate Polymers*, *84*(1), 195–202.

Wang, X. H., Guo, Y. Z., Li, D., Chen, H., & Sun, R. C. (2012). Fluorescent amphiphilic cellulose nanoaggregates for sensing trace explosives in aqueous solution. *Chemical Communications*, *48*(45), 5569–5571.

Wondraczek, H., Kotiaho, A., Fardim, P., & Heinze, T. (2011). Photoactive polysaccharides. *Carbohydrate Polymers*, *83*(3), 1048–1061.

Xu, S. Q., Lin, Y., Huang, J., Li, Z., Xu, X. J., & Zhang, L. N. (2013). Construction of high strength hollow fibers by self-assembly of a stiff polysaccharide with short branches in water. *Journal of Materials Chemistry A*, *1*(13), 4198–4206.

Yamanaka, H., Teramoto, Y., & Nishio, Y. (2013). Orientation and birefringence compensation of trunk and graft chains in drawn films of cellulose acetate-graft-PMMA synthesized by ATRP. *Macromolecules*, *46*(8), 3074–3083.

Yan, Q., Yuan, J. Y., Zhang, F. B., Sui, X. F., Xie, X. M., Yin, Y. W., et al. (2009). Cellulose-based dual graft molecular brushes as potential drug nanocarriers: stimulus-responsive micelles self-assembled phase transition behavior, and tunable crystalline morphologies. *Biomacromolecules*, *10*(8), 2033–2042.

Yang, R. M., Wang, Y. M., & Zhou, D. (2007). Novel hydroxyethylcellulose-graft-poly acrylamide copolymer for separation of double-stranded DNA fragments by CE. *Electrophoresis*, *28*(18), 3223–3231.

Yuan, W., Zhang, J., Zou, H., Shen, T., & Ren, J. (2012). Amphiphilic ethyl cellulose brush polymers with mono and dual side chains: Facile synthesis, self-assembly, and tunable temperature-pH responsivities. *Polymer*, *53*(4), 956–966.